INNOVARE JOURNAL OF MEDICAL SCIENCES

Vol 10, Issue 6, 2022

ISSN - 2321-4406

Research Article

ADME ANALYSIS AND MOLECULAR DOCKING OF PHYTOCOMPOUNDS OF *SALVIA PLEBEIA* AGAINST SIRT1 TARGETS IN LUNG CANCER

CHINMAYI KRISHNA MOORTHY*

Department of Biotechnology, NMAM Institute of Technology, Nitte, Karkala, Karnataka, India. Email: chinmayikrishnamoorthy@gmail.com

Received: 15 October 2022, Revised and Accepted: 25 October 2022

ABSTRACT

Objective: The sirtuin family is known to have a significant role in the regulation of a wide range of physiological and pathological processes, including in neurodegeneration, age-related diseases, obesity, heart disease, and cancer, according to its targets in certain signaling pathways or in particular tumors. In the present study, the counteractive activity of 10 phytocompounds of the plant *Salvia plebeia* against lung cancer's disease-causing protein SIRT1 was observed.

Methods: The molecules' structural information was obtained using PubChem and IMPPAT websites, pharmacological assessment was done using SwissADME and toxicity was predicted using ProTox-II. A computational approach was used to study the phytochemical properties of the compounds of *Salvia plebeia*. Molecular docking was done using PyRx and BIOVIA helped in the visualization process.

Results: The results from the molecular docking showed that nepetin, hispidulin, and eupatorin were the most effective against SIRT1 promoting lung cancer.

Conclusion: The compounds' ADME/T characteristics were examined to forecast their likelihood of becoming drugs. This docking study can be exploited to create powerful SIRT1 lung cancer inhibitors.

Keywords: *Salvia plebeia,* Sirtuin, Phytochemical, Drug, Pharmacological studies.

 DOI: http://dx.doi.org/10.22159/ijms.2022v10i6.46622. Journal homepage: https://innovareacademics.in/journals/index.php/ijms

INTRODUCTION

From the ancient days, people employed plants for medical purposes. The local population derives cultural and economic value from the medicinal plants utilized in modern and traditional medicine as well as in the development of medicines [1]. Traditional health-care systems are still used effectively on many fronts. The use of plant materials as a source of medicines for a broad range of human ailments has got more attention as a result of factors including population growth, inadequate drug supply, prohibitive cost of treatments, side effects of several synthetic drugs, and the development of resistance to currently used drugs for contagious diseases. Approximately 35,000 plant species have been identified as being employed as therapeutic plants thus far. Sadly, medicinal plants are continuously in danger of losing their habitats and nearing extinction owing to overexploitation, the spread of foreign invasive species, and climate change [2]. The creation of pharmacopeial, non-pharmacopeial, or synthetic medications has heavily depended on the utilization of medicinal plants as a rich supply of ingredients. Due to its high polyphenol content, *Salvia* species are frequently used in culinary and medicinal goods [3].

Salvia plebeia (Fig. 1), commonly called as Sage Weed, is native to a large area of Asia and is an annual or biennial plant. It contains a number of chemical components and is known to possess a number of pharmacological properties [4]. It grows in streamside, plains, and wet fields from sea level to 1500 m, in India. It flowers all year and grows to a height of 1.5–3 ft tall, on erect stems. The phytochemical analysis of *Salvia plebeia* contains nepetin, oleanolic acid, beta-sitosterol, secoisolariciresinol, corosolic acid, hispidulin, *Salvia coccinea,* homoplantaginin, eupatorin, ferulic acid, caffeic acid, and 12-methyltetradecanoic acid.

One of the leading causes of cancer-related deaths worldwide is lung cancer [5]. Small-cell lung cancer (SCLC) and non-small-cell lung carcinoma are the two major kinds. Surgery is mostly used to treat NSCLC and chemotherapy and radiation are often effective for treating SCLC comparatively.

The sirtuin family has come to be recognized as significant controllers of a variety of physiological and pathological processes, including lengthening of life, neurodegeneration, age-related diseases, obesity [6], heart disease [7], inflammation [8], and cancer [9]. SIRT1 is able to deacetylate a variety of non-histone substrates, including histones, that are connected to several signaling cascades. Numerous studies have revealed that depending on the targets, it interacts with in certain signaling pathways or in particular malignancies, SIRT1 may either operate as a tumor suppressor or a promoter. It has been reported that in the progression of several types of cancer, SIRT1 is involved. However, its role is not accurately understood.

The previous studies show that the silent information regulator 1 (SIRT1) gene, which is found on the long arm of chromosome 10 (10q21.3), is involved with the development of lung cancer. Given that SIRT1-mediated deacetylation inhibits the activity of a number of tumor suppressors, including p53, p73, and HIC1, it has been proposed that SIRT1 enhances the development and proliferation of tumors (Fig. 2) [10].

According to reports, the mammalian silent information regulator 1 (SIRT1) is involved in malignancies of the secretory organs, such as ovarian, thyroid, and pancreatic endocrine tumors. A recent analysis of 37 studies on malignancies looked at the relationships between SIRT1 expression and disease-free survival and overall survival. According to this study, SIRT1 overexpression was not linked with overall survival in breast, colorectal, or gastric cancers, but it was connected with a below par overall survival in liver and lung malignancies [10-14].

The main focus of this study is the utilization of bioactive substances produced from *Salvia plebeia* to treat lung cancer. These ligand

molecules engage SIRT1 in interaction. The basis of this study is the interaction between ligands and macromolecules and how well they work to prevent lung cancer.

METHODOLOGY

A thorough virtual screening and molecular docking analysis was conducted to determine the most potential therapeutic targets in the hunt for a lead that may inhibit SIRT1 activating lung cancer.

Homology modeling

The FASTA sequence of SIRT1 protein (Accession No: KAI6067711.1) was retrieved from the NCBI (National Centre for Biotechnology Information) (https://www.ncbi.nlm.nih.gov/protein) website. The FASTA sequence was uploaded in the SWISS-MODEL (https://swissmodel.expasy.org/) and the sequence alignment was carried out by BLAST which yielded a total of two models and 30 templates. The best model was selected based on the GMQE, QMEANDisCo, and Z-scores. The template 5btr.2.A was used to generate the model.

Retrieval of protein

The 3D model of SIRT1 protein was downloaded in the.pdb format from SWISS-MODEL website. The model had a sequence identity of 98.11% and QMEANDisCo score of 0.80 with respect to the template 5btr.2.A.

Protein structure analysis and purification

The downloaded protein in.pdb format was uploaded in the Zlab (https://zlab.umassmed.edu/bu/rama/index.pl) [15] server to obtain the Ramachandran plot (Fig. 3). The protein was also uploaded in pepstats (https://www.ebi.ac.uk/Tools/seqstats/emboss_pepstats/) (Table 1) [16], pepwindow (https://www.ebi.ac.uk/Tools/seqstats/emboss_pepwindow/) (Fig. 4) [17], and PDBsum (http://www.ebi.ac.uk/thorntonsrv/databases/cgibin/pdbsum/GetPage.pl?pdbcode=index.html) (Fig. 5) [18] to obtain the secondary structures and the hydropathy plot.

The BIOVIA Discovery Studio Visualizer [19] was employed to purify the protein SIRT1 by adding polar hydrogen atoms and removing ligand groups and hetero atoms. The water molecule's free energy does not correspond to its crystallographic structure. Water molecules were entirely erased before to docking since they can alter docking scores. The pre-bound ligands are taken out of the crystal structures to speed up binding with the ligands selected for the investigation. While other chains were eliminated from the protein structures to make them simpler, Chain A was kept intact for examination. To improve the quality of purified structures, polar hydrogen atoms are added. The protein went through an energy minimization process in the PyRx server [20] and was also converted to.pdbqt format.

Retrieval of ligands

The plant *Salvia plebeia* was chosen for the current study for the ligand-protein docking investigations from the IMPPAT website (https://cb.imsc.res.in/imppat/) [21]. Ligands including nepetin, oleanolic acid, beta-sitosterol, secoisolariciresinol, corosolic acid, hispidulin, *Salvia coccinea*, homoplantaginin, eupatorin, ferulic acid, caffeic acid, and

Fig. 1: *Salvia plebeia,* also known as Sage Weed

Table 1: SIRT1 protein properties obtained from pepstats

Property	Residues	Number	Mole%
Tiny	(A+C+G+S+T)	82	22.102
Small	(A+B+C+D+G+N+P+S+T+V	175	47.170
Aliphatic	(A+I+L+V)	109	29.380
Aromatic	(F+H+W+Y)	38	10.243
Non-polar	(A+C+F+G+I+L+M+P+V+W+Y)	204	54.987
Polar	(D+E+H+K+N+Q+R+S+T+Z)	167	45.103
Charged	(B+D+E+H+K+R+Z)	109	29.380
Basic	(H+K+R)	54	14.555
Acidic	(B+D+E+Z)	55	14.825

Table 2: Criteria for physicochemical properties

Properties		Optimal range
Lipophilicity	xLogP	−0.7–+5.0
Size	MW	150–500 g/mol
Polarity	TPSA	20–130
Saturation	Sp3 hybridization	Not <0.25
Flexibility	Rotatable bonds	Not more than 9

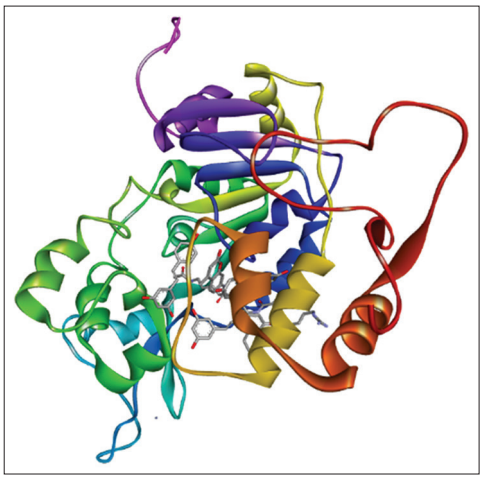

Fig. 2: 3D model of the SIRT1 protein

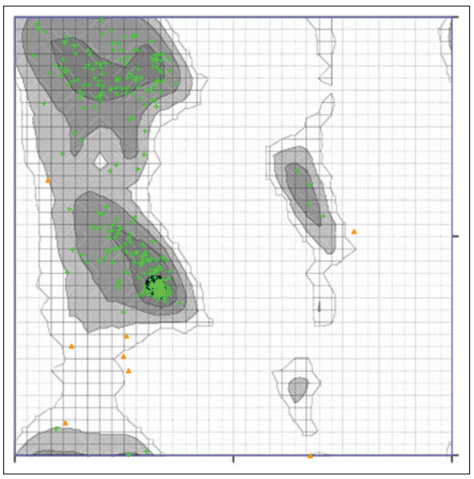

Fig. 3: Ramachandran plot of protein SIRT1 using Zlab

12-methyltetradecanoic acid were chosen based on their medicinal and therapeutic applications. Using PubChem (https://pubchem.ncbi.nlm.nih.gov/) databases, the canonical SMILES and SDF structures were retrieved and the physicochemical characteristics of the ligand were examined.

Drug likeness of ligands and pharmacological studies

Adsorption, distribution, metabolism, excretion, and toxicity (ADMET) is the foremost properties that determine if a chemical is a potential drug. SwissADME (http://www.swissadme.ch/index.php) [22] (Tables 3 and 5) server was used to examine the pharmacological properties of the 10 ligands. The size, flexibility, unsaturation, lipophilicity, polarity, and insolubility were assessed as per the parameters listed in Table 2. Then, the Lipinski rule of 5 was used to choose the top ligands (Table 4). To study ligand aggregation, ChemAGG (https://admet.scbdd.com/ChemAGG/index/) (Table 6) [23] was used. ProTox-II [24] was employed to evaluate the toxicological traits (Table 7). Physicochemical and pharmacokinetic examination was completed by producing a BOILED-Egg (Fig. 6) model in the SwissADME server.

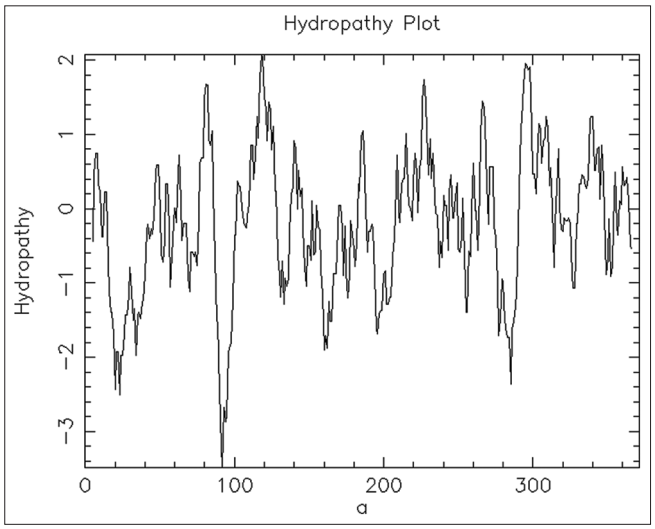

Fig. 4: Hydropathy plot of SIRT1

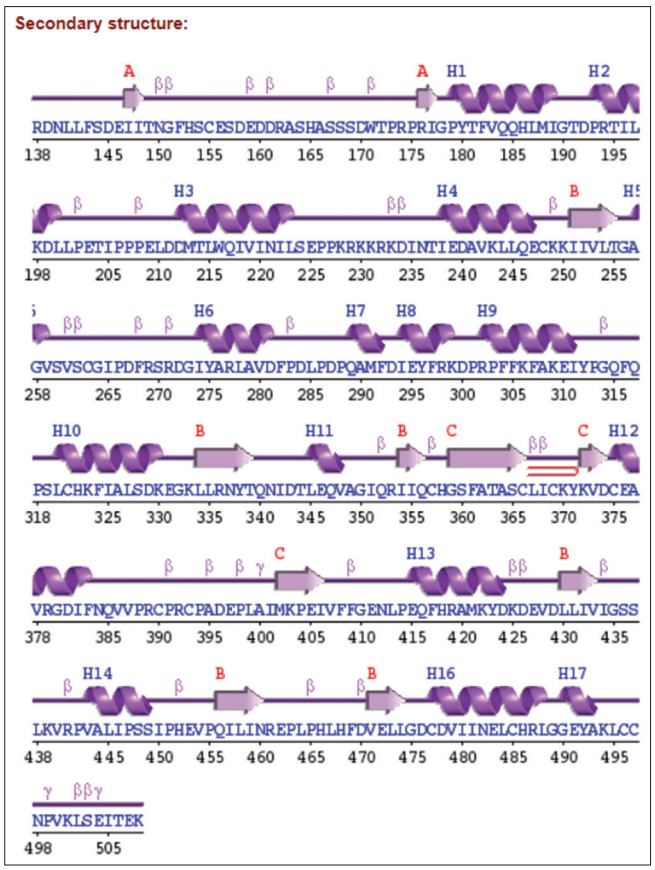

Fig. 5: Secondary structure of protein SIRT1

Molecular docking studies

Molecular docking studies are employed to examine the inhibition effect or the interaction of the ligand with the targeted protein. For the molecular docking studies, PyRx server was used. The purified protein was converted to AutoDock.pdbqt format and the ligands were uploaded using the Open Babel option. The ligands were subjected to energy minimization by applying universal force filed (_uff). Energy minimization also aids in the removal of salt entities that might be present in the sdf structures of the ligand molecules. Further, the prepared ligands were converted to AutoDock.pdbqt format and the grid was generated with the dimensions x=57.44801, y=73.9049, and z=71.2009. By default, the PyRx software assumes the proteins (macromolecules) as rigid and the ligands as flexible. Therefore, the ligands undergo nine different conformational changes to attain the best possible interactions with the protein. The docking interactions are analyzed with respect to the binding affinity. The least binding affinity corresponds to the best docking interactions. Top 3 ligands were selected and docked separately against the SIRT1 protein (Table 8).

Visualization

The best complexes were visualized in the DS BIOVIA Discovery Studio at the protein- ligand interaction interface. The bond angle, bond type, and the molecular interaction were studied with 2D and 3D interactions diagrams which provide valuable insights about the protein-ligand interactions (Figs. 7-9).

RESULTS

Protein structure analysis

Black, dark gray, gray, and light gray represent highly preferred conformation. Delta ≥ −2
White with black grid represents preferred conformations. −2 > Delta ≥ −4
White with gray grid represents questionable conformations. Delta < −4
Highly preferred observations shown as GREEN crosses: 313 (97.508%)
Preferred observations shown as BROWN triangles: 8 (2.492%)
Questionable observations show as RED circles: 0 (0.000%)

Hydropathy plot

EMBOSS pepwindow was used to obtain the hydropathy plot. The amino acid residue is plotted on the X-axis of the hydropathy plot shown and the hydrophilicity is plotted on the Y-axis.

Secondary structure

The secondary structure of the protein SIRT1 was obtained using the PDBsum website. The secondary structure of SIRT1 contains three sheets, three beta-alpha-beta units, one beta hairpin, three beta bulges, 11 strands, 17 helices, 16 helix-helix interacts, 34 beta turns, and three gamma turns.

Protein statistics

The frequency of each amino acid residue in the protein sequence under a certain attribute is displayed in the protein statistics. EMBOSS pepstats was used to obtain statistical data on the amino acids under conditions, such as size, charge, and pH.

The protein structure had a total of 371 amino acid residues. The isoelectric point was found to be 5.4609. The average molecular weight was 42092.60. The average residue weight was 113.457.

SwissADME analysis

Given below are the pharmacological properties of the selected 10 ligands. The ligands highlighted in red do not fulfill the required criteria.

Table 3: Physicochemical properties of the ligand molecules

Ligand	Molecular weight	Fraction Csp3	Rotatable bonds	TPSA	Lipophilicity
Nepetin	316.26	0.06	2	120.36	2.5
Oleanolic acid	456.7	0.9	1	57.53	7.49
Beta-sitosterol	414.71	0.93	6	20.23	9.34
Secoisolariciresinol	362.42	0.4	9	99.38	2.52
Corosolic acid	472.7	0.9	1	77.76	6.37
Hispidulin	300.26	0.06	2	100.13	2.99
Homoplantaginin	462.4	0.32	5	179.28	0.83
Eupatorin	344.32	0.17	4	98.36	3.4
Ferulic acid	194.18	0.1	3	66.76	1.51
Caffeic acid	180.16	0	2	77.76	1.15

Table 4: Evaluation of Lipinski filter analysis

Ligand	Molecular weight	MLogP	H acceptors	H donors	Molar refractivity
Nepetin	316.26	−0.31	7	4	82.5
Oleanolic acid	456.7	5.82	3	2	136.65
Beta-sitosterol	414.71	6.73	1	1	133.23
Secoisolariciresinol	362.42	1.56	6	4	99.28
Corosolic acid	472.7	4.97	4	3	138.08
Hispidulin	300.26	0.22	6	3	80.48
Homoplantaginin	462.4	−1.89	11	6	112.6
Eupatorin	344.32	0.17	7	2	91.44
Ferulic acid	194.18	1	4	2	51.63
Caffeic acid	180.16	0.7	4	3	47.16

Table 5: ADME analysis

Ligands	BBB barrier	GI absorption	PGP substrate	Solubility (LOGSw-SILICOS IT)	Silicos-IT solubility (mg/ml)
Nepetin	0.002	0.067	0.581	−3.94	3.65E-02
Oleanolic acid	0.694	0.022	0	−6.12	3.45E-04
Beta-sitosterol	0.84	0.004	0.001	−6.19	2.69E-04
Secoisolariciresinol	0.039	0.459	0.074	−4.54	1.05E-02
Corosolic acid	0.739	0.04	0	−4.85	6.68E-03
Hispidulin	0.004	0.017	0.928	−4.52	9.07E-03
Homoplantaginin	0.185	0.764	0.907	−2.79	7.48E-01
Eupatorin	0.01	0.024	0.01	−5.33	1.63E-03
Ferulic acid	0.329	0.03	0.086	−1.42	7.43E+00
Caffeic acid	0.119	0.009	0.024	−0.71	3.51E+01

Table 6: Aggregation analysis

Compound	Probability score	Aggregator class
Nepetin	0.139	0
Oleanolic acid	0.003	0
Beta-sitosterol	0.031	0
Secoisolariciresinol	0.01	0
Corosolic acid	0.003	0
Hispidulin	0.075	0
Homoplantaginin	0.009	0
Eupatorin	0.072	0
Ferulic acid	0.053	0
Caffeic acid	0.025	0

Lipinski analysis
Criteria for Lipinski filter: H bond donor's ≤5, H bond acceptors i filter: H bond donor's ≤ulesculesele the range of 150–500 g/mol.

Ligands nepetin, secoisolariciresinol, hispidulin, eupatorin, ferulic acid, and caffeic acid fulfill the Lipinski criteria. Whereas, oleanolic acid, beta-sitosterol, and homoplantaginin do not fulfill the criteria.

ADME analysis
Blood–brain barrier restricts the penetration of the compound into the brain. Gastrointestinal adsorption should be high to improve the drug's efficiency. The solubility values need to be less negative. These values are obtained using SwissADME.

Aggregation analysis
Compounds were classified as aggregators and non-aggregators using the ChemAGG server. Compounds with probability score 0 are impossible to aggregate.

Toxicity analysis
LD50 is the amount of substance, administered all at once which can also lead to the death of animals. LD50 values <50 mg/kg are known to be highly toxic.

Boiled-Egg analysis
The egg yolk offers a significant potential for brain invasion, whereas the white part (egg white) suggests a higher possibility of passive absorption through the GI tract. The yolk and white parts are not exclusive to one another.

In this study, oleanolic acid, beta-sitosterol, and homoplantaginin fall outside the plot and so they are not considered for further studies.

Molecular docking analysis
The ligands nepetin, hispidulin, and eupatorin had a higher binding affinity of −7.9, −7.8, and −7.8, respectively, with SIRT1.

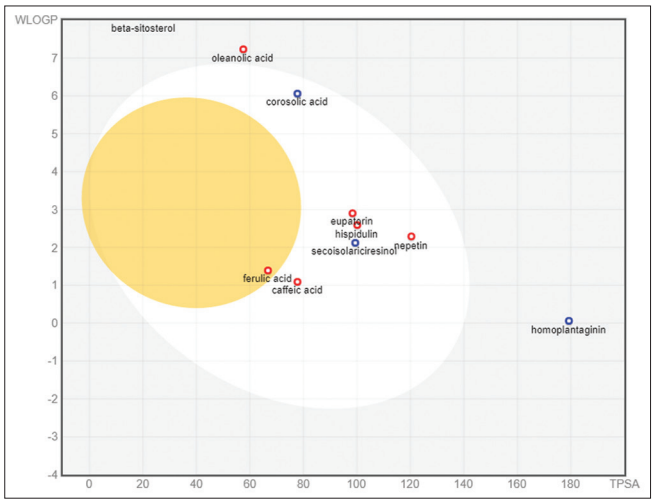

Fig. 6: Boiled-egg analysis for GI absorption and blood–brain barrier penetration

Table 7: Toxicity analysis

Compound	Predicted LD50 (mg/kg)	Predicted toxicity class
Nepetin	3919	5
Oleanolic acid	2000	4
Beta-sitosterol	890	4
Secoisolariciresinol	2000	4
Corosolic acid	2000	4
Hispidulin	4000	5
Homoplantaginin	5000	5
Eupatorin	4000	5
Ferulic acid	1772	4
Caffeic acid	2980	5

Table 8: SIRT1 docking score with selected ligands

Ligand	Binding affinity
Oleanolic acid	−9.7
Beta-sitosterol	−8.2
Ferulic acid	−5.9
Hispidulin	−7.8
Nepetin	−7.9
Homoplantaginin	−8.4
Secoisolariciresinol	−6.6
Caffeic acid	−5.8
Corosolic acid	−8.7
Eupatorin	−7.8

The ligands with higher binding affinity were ignored because they did not fit the Lipinski criteria and pass the BOILED-Egg analysis.

Visualization

Molecular interaction of the ligand nepetin with protein SIRT1

The amino acids isoleucine, serine, cystine, phenylalanine, leucine, histidine, glutamic acid, alanine, and arginine take part in this interaction between the ligand nepetin and the protein SIRT1.

The category of bonds are hydrogen and hydrophobic.

The types of bonds formed are four conventional hydrogen bond, 1 Pi Pi T shaped, 1 alkyl, and 1 Pi-alkyl. The distances between the ligand and the protein at various sites were 2.18951, 2.16618, 2.38683, 2.53267, 5.01766, 4.1283, and 5.37122.

Molecular interaction of the ligand hispidulin with SIRT1

The amino acids isoleucine, serine, cystine, phenylalanine, leucine, histidine, glutamic acid, alanine, and arginine take part in this interaction between the ligand hispidulin and the protein SIRT1.

The categories of bonds are four hydrogen and three hydrophobic.

The types of bonds formed are the five conventional hydrogen bond, 1 Pi Pi T shaped, 1 alkyl, and 2 Pi-alkyl. The distances between the ligand and the protein at various sites were 2.20014, 2.36454, 2.51861, 2.8523, 2.14449, 4.90697, 4.26485, 5.44591, and 5.30901.

Molecular interaction of the ligand eupatorin with SIRT1

The amino acids lysine, arginine, glutamine, aspartic acid, glutamic acid, proline, alanine, phenylalanine, threonine, and leucine take part in this interaction between the ligand eupatorin and the protein SIRT1.

The category of bonds are five hydrogen and eight hydrophobic. The types of bonds formed are the four conventional hydrogen bond, 1 Pi-Sigma, 1 Pi Pi stacked, Pi-Pi T shaped, 3 alkyl, and 2 Pi-alkyl. The distances between the ligand and the protein at various sites were 2.37147, 2.34906, 2.74258, 2.1725, 3.61487, 3.51063, 3.83539, 4.69093, 5.1144, 4.57833, 5.00783, 4.34446, 4.76652, and 5.24049.

DISCUSSION

In the present study, the phytocompounds of *Salvia plebeia*, which are nepetin, oleanolic acid, beta-sitosterol, secoisolariciresinol, corosolic acid, hispidulin, *Salvia coccinea*, homoplantaginin, eupatorin, ferulic acid, caffeic acid, and 12-methyltetradecanoic acid were taken as ligands and their interaction with purified SIRT1 protein was examined.

It was observed through the analysis of physicochemical properties and various other mentioned criteria that nepetin, hispidulin, and eupatorin worked best in inhibiting the cancer promoting properties of the SIRT1 protein. This could lead to the discovery of therapeutic drugs that could inhibit lung tumors promoted by the SIRT1 protein.

Due to their possible anticancer efficacy and minimal toxicity, natural compounds have become more and more popular. Protein tyrosine phosphatase 1B (PTP1B) is linked to dendritic cell-based cancer immunotherapy and has been approved as a target for therapeutic intervention in diabetes and obesity. Moreover, mounting evidences show that PTP1B has a role in the development of several malignancies.

Earlier research show evidence that nepetin inhibits the catalytic activity of PTPN1, PTPN2, and PTPN11 which act as tumor promoters in prostate cancer, colorectal cancer, gastric cancer, and non-small cell lung cancer and hepatocellular carcinoma [25].

Hispidulin has several biological effects, most notably anti-inflammatory, antiplatelet, anticonvulsant, and anticancer ones. Hispidulin has been proven in studies to have an impact on cell proliferation, apoptosis, cell cycle, and metastasis as a possible anticancer medication. In addition, when taken with several popular clinical anticancer medications, hispidulin displays anti-tumor benefits. It may be said that hispidulin has a great deal of potential to be an important supplemental therapy for the treatment and prevention of cancer [26]. In addition, through increasing the expression of cleaved caspase-3 and cleaved poly (ADP-ribose) polymerase, hispidulin caused cell death in non-small-cell lung cancer (NSCLC) cells. The theoretical underpinnings for hispidulin anticancer effects in NSCLC were revealed in earlier research [27].

Breast cancer cell lines was used in an investigation on eupatorin ability to induce cell death and reduce cancer cell growth. The activity of pro-apoptotic and anti-survival genes was regulated by eupatorin, which prevented metastasis in the cells. Eupatorin cytotoxicity was also restricted to cancer cells, sparing healthy human breast cells from damage [28].

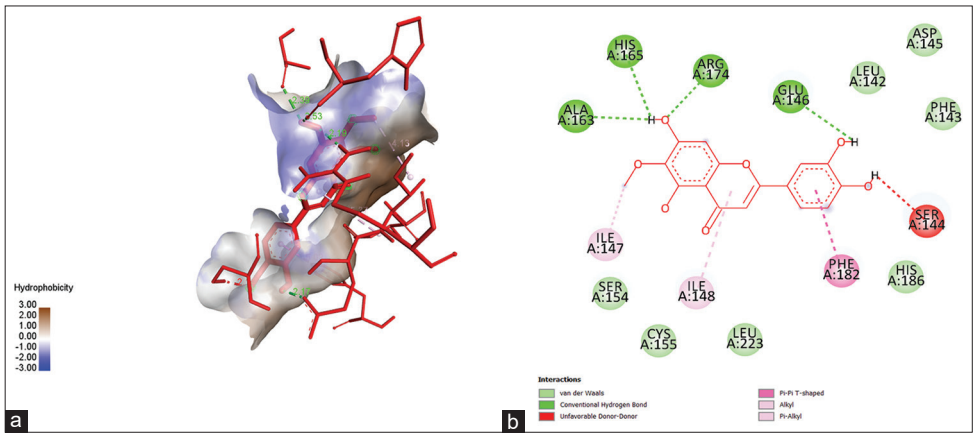

Fig. 7: Visualization of interaction of nepetin with SIRT1. (a) 3D interaction, (b) 2D interaction

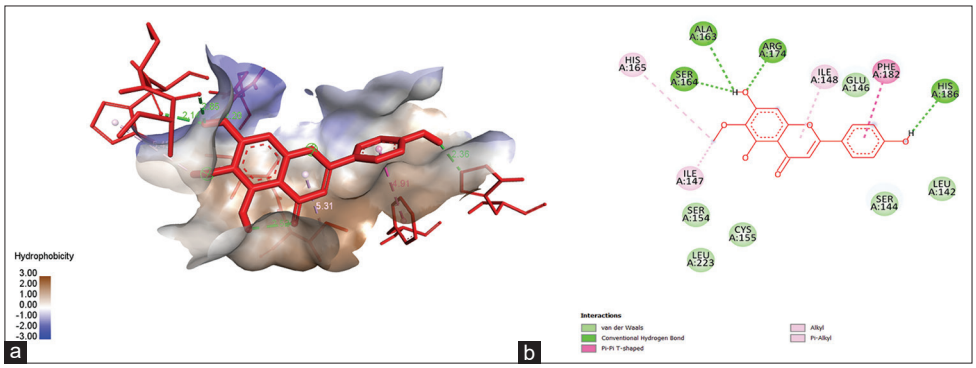

Fig. 8: Visualization of interaction of hispidulin with SIRT1. (a) 3D diagram, (b) 2D diagram

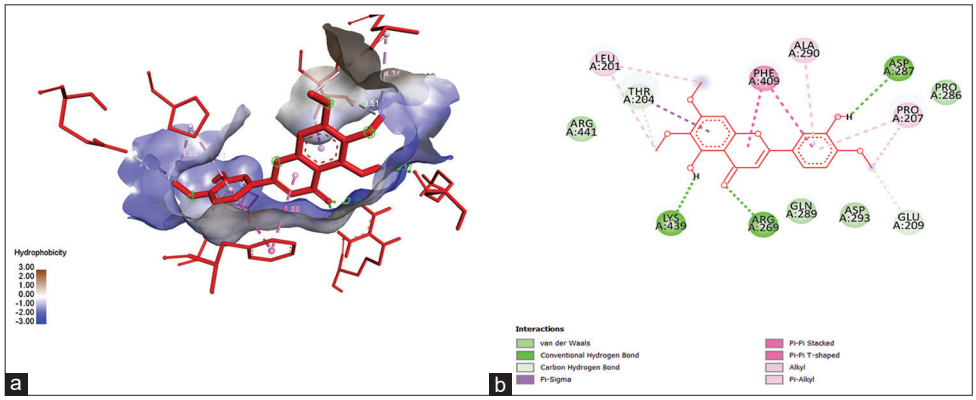

Fig. 9: Visualization of interaction of eupatorin with SIRT1. (a) 3D interaction. (b) 2D interaction

The effective treatment of cancer patients has been significantly assisted by the discovery of anticancer medicines derived from therapeutic herbs. In addition, by isolating the active components from medicinal plants and converting them into pharmaceuticals, they have been utilized as folk remedies and anticancer materials. Various biological resources, including medicinal herbs, have been evaluated for the formulation of anticancer medications to combat the establishment of anticancer drug resistance, and their significance is growing [28]. From earlier research, it is known that *Salvia plebeia* and its phytocompounds blocked the interaction between PD-1 (programmed cell death 1) and PD-L1 (programmed cell death-ligand 1) in the molecular level. *Salvia plebeia* is also known to increase CD8+ T-cells (cytotoxic T lymphocytes) in tumors through the activation of tumor-specific T-cells and thereby resulting in the inhibition of tumor growth [29].

The leading factor in cancer-related deaths globally is lung cancer. The quick discovery of innovative therapy drugs for all cancer subtypes, including lung cancer, has been growing by recent developments in molecular diagnostics. The protein SIRT1 acts as both, a tumor promoter and tumor suppressor. SIRT1 has acted as a promoter in some cancer cells such as primary colon, prostate, acute myeloid leukemia, and melanoma and its downregulation was observed in breast cancer and hepatic cell carcinomas. In the present study, we observe the interaction between plant ligands with SIRT1 promoting lung cancer. It was also observed that SIRT1 overexpression was associated with a worse overall survival in lung and liver cancer [29,30].

The best model of the protein SIRT1 was selected based on the QMEANDisCo score from the SWISS-MODEL website and was downloaded in the.pdb format. The protein was purified using the BIOVIA server. The protein also went through an energy minimization process and was converted to.pdbqt format. All the selected 10 ligands of the plant *Salvia plebeia*, obtained from the IMPPAT website, were docked against the purified protein using the PyRx server. The best

three ligands were selected based on their binding affinities. Nepetin, hispidulin, and eupatorin had binding affinity values −8.2, −7.8, and −7.8, respectively. The other ligands either did not fit into the fixed criteria or had lower binding affinities.

The three ligands were visualized in the BIOVIA server and their hydrophobic interactions, distances between bonds, and the types of bonds were observed. Because nepetin had the best binding affinity of −7.8 and fit into all the criteria, it was known that that ligand was the most suitable phytocompound against SIRT1 promoting lung cancer.

CONCLUSION

Ten bioactive compounds were selected from the plant *Salvia plebeia* based on their pharmacological properties. Out of these, the ligands nepetin, hispidulin, and eupatorin had a higher binding affinity of −8.2, −7.8, and −7.8, respectively, with SIRT1. Dassault Systemes BIOVIA Discovery Studio was used for the visualization of the interactions. The visualization of the docked structures proved that nepetin had better binding with the receptors.

ACKNOWLEDGMENT

I thank BioNome Pvt. Ltd., Bengaluru, India, for providing all the guidance and support required.

REFERENCES

1. Rahman H, Roy B, Chowdhury GM, Hasan A, Saimun S. Medicinal plant sources and traditional healthcare practices of forest-dependent communities in and around Chunati Wildlife Sanctuary in Southeastern Bangladesh. Environ Sustain 2022;5:207-41.
2. Xia C, Huang Y, Qi Y, Yang X, Xue T, Hu R, *et al*. Developing long-term conservation priority planning for medicinal plants in China by combining conservation status with diversity hotspot analyses and climate change prediction. BMC Biol 2022;20:89.
3. Wang J, Xu J, Gong X, Yang M, Zhang C, Li M. Biosynthesis, chemistry, and pharmacology of polyphenols from Chinese *Salvia* species: A review. Molecules 2019;24:155.
4. Liang YY, Wan XH, Niu FJ, Xie SM, Guo H, Yang YY, *et al*. *Salvia plebeia* R. Br.: An overview about its traditional uses, chemical constituents, pharmacology and modern applications. Biomed Pharmacother 2020;121:109589.
5. Tran NH, Kisiel J, Roberts LR. Using cell-free DNA for HCC surveillance and prognosis. JHEP Rep 2021;3:100304.
6. Subbaramaiah K, Iyengar NM, Morrow M, Elemento O, Zhou XK, Dannenberg AJ. Prostaglandin E_2 down-regulates sirtuin 1 (SIRT1), leading to elevated levels of aromatase, providing insights into the obesity-breast cancer connection. J Biol Chem 2019;294:361-71.
7. Sun S, Wang C, Weng J. MicroRNA-138-5p drives the progression of heart failure via inhibiting sirtuin 1 signaling. Mol Med Rep 2021;23:276.
8. Lv Y, Lin S, Peng F. SIRT1 gene polymorphisms and risk of lung cancer. Cancer Manag Res 2017;9:381-6.
9. Hosseninia S, Ameli A, Aslani MR, Pourfarzi F, Ghobadi H. Serum levels of sirtuin-1 in patients with lung cancer and its association with karnofsky performance status. Acta Biomed 2021;92:e2021012.
10. Wang C, Yang W, Dong F, Guo Y, Tan J, Ruan S, *et al*. The prognostic role of Sirt1 expression in solid malignancies: A meta-analysis. Oncotarget 2017;8:66343-51.
11. Wu S, Jiang J, Liu J, Wang X, Gan Y, Tang Y. Meta-analysis of SIRT1 expression as a prognostic marker for overall survival in gastrointestinal cancer. Oncotarget 2017;8:62589-99.
12. Tang BL. Sirt1's systemic protective roles and its promise as a target in antiaging medicine. Transl Res 2011;157:276-84.
13. Waterhouse A, Bertoni M, Bienert S, Studer G, Tauriello G, Gumienny R, *et al*. SWISS-MODEL: Homology modelling of protein structures and complexes. Nucleic Acids Res 2018;46:W296-303.
14. Pott PC, Hoffmann JP, Stiesch M, Eisenburger M. Polish of interface areas between zirconia, silicate-ceramic, and composite with diamond-containing systems. J Adv Prosthodont 2018;10:315-20.
15. Imholte G, Sauteraud R, Gottardo R. Analyzing peptide microarray data with the R pepStat package. Methods Mol Biol 2016;1352:127-42.
16. Li W, Cowley A, Uludag M, Gur T, McWilliam H, Squizzato S, *et al*. The EMBL-EBI bioinformatics web and programmatic tools framework. Nucleic Acids Res 2015;43:W580-4.
17. Laskowski RA, Jabłońska J, Pravda L, Vařeková RS, Thornton JM. PDBsum: Structural summaries of PDB entries. Protein Sci 2018;27:129-34.
18. Jejurikar BL, Rohane SH. Drug designing in discovery studio. Asian J Res Chem. 2021;14(2):135–8.
19. Deenadayalan A, Vijayalakshmi S, Janaki CS, Jayaraman S. Molecular docking analysis of stevioside with Akt and PPARγ. Bioinformation 2021;17:283-8.
20. Mohanraj K, Karthikeyan BS, Vivek-Ananth RP, Chand RP, Aparna SR, Mangalapandi P, *et al*. IMPPAT: A curated database of Indian medicinal plants, phytochemistry and therapeutics. Sci Rep 2018;8:4329.
21. Daina A, Michielin O, Zoete V. SwissADME: A free web tool to evaluate pharmacokinetics, drug-likeness and medicinal chemistry friendliness of small molecules. Sci Rep 2017;7:42717.
22. Yang ZY, Yang ZJ, Dong J, Wang LL, Zhang LX, Ding JJ, *et al*. Structural analysis and identification of colloidal aggregators in drug discovery. J Chem Inf Model 2019;59:3714-26.
23. Banerjee P, Eckert AO, Schrey AK, Preissner R. ProTox-II: A webserver for the prediction of toxicity of chemicals. Nucleic acids Res 2018;46:W257-63.
24. Xu Q, Wu N, Li X, Guo C, Li C, Jiang B, *et al*. Inhibition of PTP1B blocks pancreatic cancer progression by targeting the PKM2/AMPK/mTOC1 pathway. Cell Death Dis 2019;10:874.
25. Liu K, Zhao F, Yan J, Xia Z, Jiang D, Ma P. Hispidulin: A promising flavonoid with diverse anti-cancer properties. Life Sci 2020;259:118395.
26. Lv L, Zhang W, Li T, Jiang L, Lu X, Lin J. Hispidulin exhibits potent anticancer activity *in vitro* and *in vivo* through activating ER stress in non-small-cell lung cancer cells. Oncol Rep 2020;43:1995-2003.
27. Razak NA, Yeap SK, Alitheen NB, Ho WY, Yong CY, Tan SW, *et al*. Eupatorin suppressed tumor progression and enhanced immunity in a 4t1 murine breast cancer model. Integr Cancer Ther 2020;19:1534735420935625.
28. Choi JG, Kim YS, Kim JH, Kim TI, Li W, Oh TW, *et al*. Anticancer effect of *Salvia plebeia* and its active compound by improving T-cell activity via blockade of PD-1/PD-L1 interaction in humanized PD-1 mouse model. Front Immunol 2020;11:598556.
29. Alves-Fernandes DK, Jasiulionis MG. The role of SIRT1 on DNA damage response and epigenetic alterations in cancer. Int J Mol Sci 2019;20:3153.
30. Frazzi R. SIRT1 in secretory organ cancer. Front Endocrinol 2018;9:569.